Optical spectroscopy of Nd^{3+} in the $Bi_{12}SiO_{20}$ piezoelectric crystal

1999 J. Phys.: Condens. Matter 11 3201

(http://iopscience.iop.org/0953-8984/11/15/026)

J. Phys.: Condens. Matter **11** (1999) 3201–3207. Printed in the UK PII: S0953-8984(99)99033-1

Optical spectroscopy of Nd^{3+} in the $Bi_{12}SiO_{20}$ piezoelectric crystal

F Ramos L†, D Jaque‡, J Romero†, J García Solé‡ and U Caldiño G†

† Departamento de Física, Universidad Autónoma Metropolitana, Iztapalapa, PO Box 55-534, 09340 México, DF, México

‡ Departamento de Física de Materiales C-IV, Universidad Autónoma de Madrid, Cantoblanco 28049, Madrid, Spain

Received 6 November 1998

Abstract. A systematic investigation of luminescence and optical absorption of the Nd^{3+} ion in the $Bi_{12}SiO_{20}$:Nd^{3+} crystal is presented. Most Stark energy levels have been identified. The Judd–Ofelt theory is applied to measured values of absorption line strengths to obtain the intensity parameters: Ω_2, Ω_4 and Ω_6. These parameters are used to calculate the absorption line strengths, as well as the radiative lifetime and the branching ratios from the metastable $^4F_{3/2}$ state to the ^4I_J manifolds. The relevant spectroscopic parameters for laser applications: emission cross section and quantum efficiency, were then estimated. The spectroscopic quality factor (Ω_4/Ω_6) calculated is in agreement with those of other Nd^{3+} based laser crystals.

1. Introduction

The study of the optical properties of Nd^{3+} in electro-optic oxide single crystals has received considerable attention in recent years [1–3]. Neodymium, which is the most common activator in laser crystals, emits an intense luminescence, and this is of considerable interest in quantum electronics and its applications.

Recently, the interest in the $Bi_{12}SiO_{20}$ piezoelectric crystal doped with Nd^{3+} ions (BSO:Nd) has arised because of its potential to be grown more easily and economically due to its lower melting point ($\sim$880 °C) [3, 4]. In addition, BSO has favourable photo-conductive, photo-refractive, electro-optic and magneto-optic properties for the laser light control. Moreover, the ionic radius of Bi^{3+} (0.96 Å) is similar to that of Nd^{3+} (0.99 Å). All these characteristics make the BSO crystal a potential material for laser action.

In this paper we present a systematic investigation of luminescence and optical absorption spectra of Nd^{3+} in BSO, at low (11 K) and room temperature (RT), in order to identify most Stark energy levels of Nd^{3+} in this crystal, as well as to apply the Judd–Ofelt (JO) analysis. This theory has been for more than 30 years a standard method for calculating the parity forbidden electric-dipole (ED) radiative transition rates between various levels of rare-earth ions in crystalline and glassy hosts. Thus, we have determined the well known intensity parameters Ω_2, Ω_4 and Ω_6 ($\Omega_{2,4,6}$), which characterize the effect of the host crystal on the Nd^{3+} transitions. Such parameters allowed us to calculate the radiative lifetime and the branching ratios from the Nd^{3+} $^4F_{3/2}$ metastable state to the ^4I_J manifolds, which were then used to estimate the relevant laser parameters (quantum efficiency and emission cross section) for the main laser channel $^4F_{3/2} \rightarrow {}^4I_{11/2}$.

0953-8984/99/153201+07$19.50

Analysis of photoluminescence and absorption spectra of BSO:Nd, previously performed [3], revealed that the Nd^{3+} ion forms two different non-equivalent centres in this compound. Considering that the peak position of the emission and absorption lines are associated with two non-equivalent centres, then the energy levels here reported can be considered as average values of such centres.

2. Experiment

The BSO crystals doped with 0.01 at.% of Nd^{3+} were grown from the melt by the Czochralski technique using platinum crucibles. The RT absorption spectra were recorded on a Milton Roy Spectronic 3000 array spectrophotometer. The emission spectra were acquired by exciting the sample with a CW Ti:sapphire laser (Spectra Physics 3900) pumped by an Ar^{+} laser (SP-2020). Emission from the crystal was dispersed by a 500 H SPEX monochromator (spectral resolution $\sim$0.05 nm), and detected with a cooled Ge detector. The signals were recorded using a SR400 two-channel gated photon counter. Monochromator control and data acquisition for both excitation and emission spectra were performed with an IBM PS/2 computer. Low temperature measurements (11 K) were carried out using a closed-cycle helium cryostat.

3. Experimental results and discussion

Figure 1 shows the absorption spectrum at 11 K of Nd^{3+} in BSO:Nd. It consists of a number of groups of lines corresponding to transitions between the ground state $^4I_{9/2}$ and higher-energy states inside the $4f^3$ electronic configuration of the Nd^{3+} ion. An assignment of Stark energy levels associated with such lines was possible because, at this temperature, thermalization effects are drastically reduced, and then, the optical spectrum appears greatly simplified. Table 1 lists the identified energy levels up to 20 000 cm^{-1}. At higher energies the absorption edge becomes so dominant that no more states can be accessed. The RT absorption spectrum is similar to that at 11 K, except by an additional line broadening and the presence of some weak lines, at the low-energy side of each transition, associated with thermal population of the ground state $^4I_{9/2}$ excited levels.

Table 1. Energy levels of the Nd^{3+} ion in BSO:Nd.

Multiplets	Energy (cm^{-1})
$^4I_{9/2}$	0; 130; 272; 406; 541
$^4I_{11/2}$	1364; 1497; 1593; 1659; 1732; 1788
$^4I_{13/2}$	3292; 3430; 3545; 3595
$^4F_{3/2}$	11 248; 11 520
$^4F_{5/2}$, $^2H_{9/2}$	12 285; 12 315; 12 406; 12 453; 12 531; 12 562; 12 706; 12 738
$^4F_{7/2}$, $^4S_{3/2}$	13 210; 13 245; 13 386; 13 477; 13 513; 13 568
$^4F_{9/2}$	14 471; 14 641; 14 705; 14 814
$^2H_{11/2}$	15 822
$^4G_{5/2}$, $^2G_{7/2}$	16 778; 16 920; 17 064; 17 152; 17 241; 17 271; 17 361
$^2G_{3/2}$, $^4G_{7/2}$, $^4G_{9/2}$, $^2K_{13/2}$	18 691; 18 726; 18 832; 18 939; 19 047; 19 342; 19 370; 19 421; 19 440

Figure 2 displays the 11 K emission spectrum from the $^4F_{3/2}$ level to the three lower manifolds $^4I_{9/2}$, $^4I_{11/2}$ and $^4I_{13/2}$ ($^4I_{9/2,11/2,13/2}$). This spectrum allowed us to determine the energy levels of such terminal states (see table 1), which were not accessible from the absorption spectrum. The number of lines for the emissions $^4F_{3/2} \rightarrow {}^4I_{9/2}$ and $^4I_{11/2}$ corresponds to

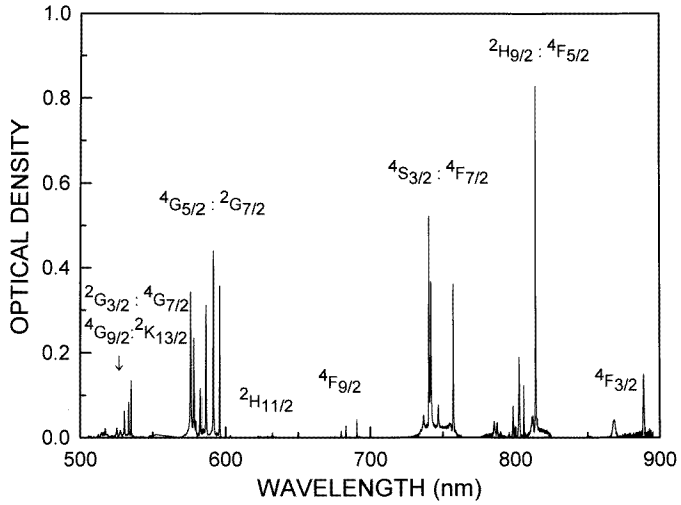

Figure 1. 11 K absorption spectrum of Nd^{3+} in BSO:Nd. The crystal absorption edge has been removed.

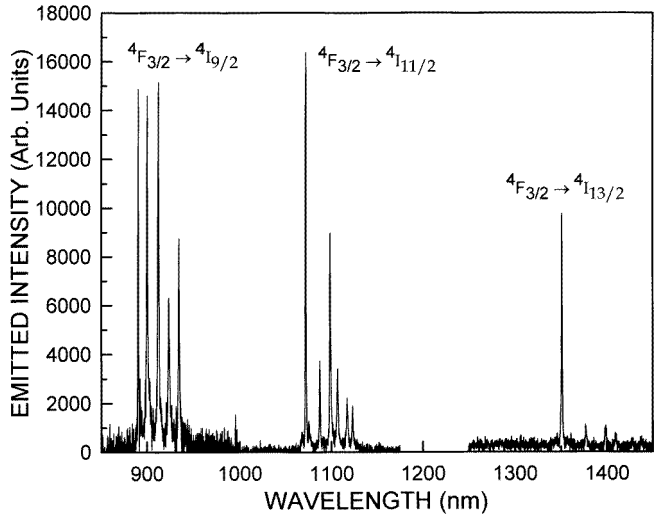

Figure 2. 11 K emission spectrum in the infrared region obtained under excitation at 800 nm.

that predicted by theory for the Nd^{3+} ion in crystal fields of symmetry below cubic. The Stark structure of the multiplet $^4I_{13/2}$ was difficult to analyse because of the low emission intensity in some of its levels. The emission $^4F_{3/2} \rightarrow {}^4I_{15/2}$ was not accessible to our detectors.

Now the JO theory can be applied in order to estimate the laser relevant spectroscopic parameters (emission cross section and quantum efficiency). The most relevant absorption transitions involved in the JO analysis are displayed in the RT detailed absorption spectra of figure 3. Considering that the RT absorption lines are thermally broadened and have, moreover, associated hot side bands originated from population in the ground state $^4I_{9/2}$ excited levels, then the JO assumption of equal population for all the states of same J is fulfilled.

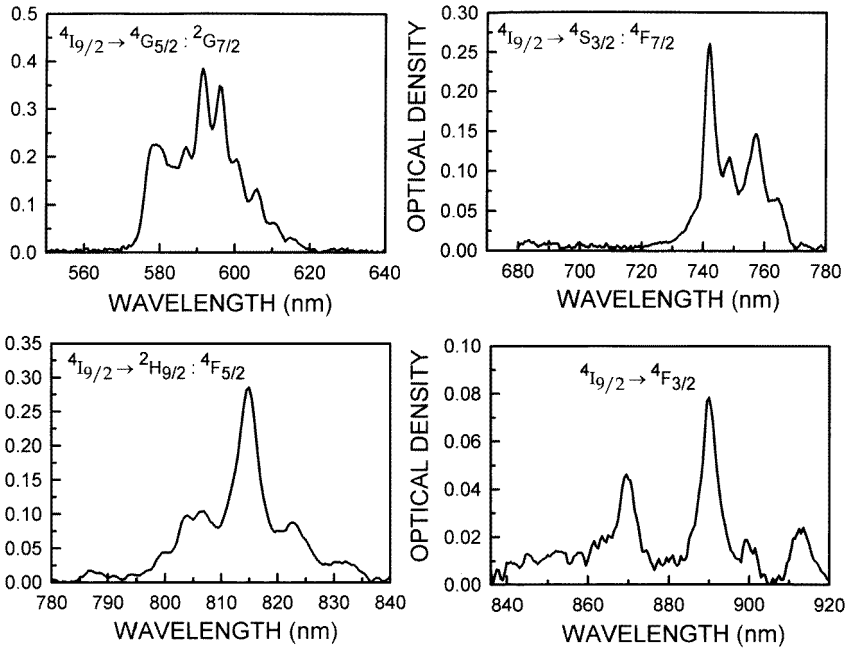

Figure 3. RT detailed absorption spectra for the transitions taken to determine the JO intensity parameters in BSO:Nd.

Measured absorption line strengths were obtained from the RT acquired absorption spectra using the following expression:

$$S_{meas}(J \rightarrow J') = \frac{3ch(2J+1)}{8\pi^3 N_0 \bar{\lambda} e^2} \frac{9n}{(n^2+1)^2} \Gamma \tag{1}$$

where J and J' are the angular momentum quantum numbers of the initial and final states, respectively, $(2J + 1)$ is the multiplicity of the ground state ($J = 9/2$), N_0 is the Nd^{3+} concentration in the host (4.5×10^{18} ions cm^{-3}), $\bar{\lambda}$ is the mean wavelength of the absorption band, n is the refractive index of the sample at the wavelength $\bar{\lambda}$, and Γ the integrated absorbance measured for each ED particular transition $J \rightarrow J'$. The wavelength dependence of n was estimated from the Sellmeier dispersion equation:

$$n = \left[1 + \frac{A\lambda^2}{\lambda^2 - B}\right]^{1/2} \tag{2}$$

where the values for $A = 2.278$ and $B = 11\,420$ nm^2 were taken from those estimated previously [5] for the YAG. A computer program was used to evaluate Γ numerically for each absorption band. When two or more absorption manifolds were found to be overlapped, the total integrated absorbance of the manifolds was treated as a single experimental point.

The absorption line strength for an ED transition can be expressed in terms of the $\Omega_{2,4,6}$ intensity parameters. According to JO theory [6, 7]:

$$S_{calc}(J \rightarrow J') = \sum_{t=2,4,6} \Omega_t |\langle (S, L)J||U^{(t)}||(S', L')J'\rangle|^2 \tag{3}$$

where the reduced matrix elements $\langle \ldots||U^{(t)}||\ldots\rangle$ are the unitary tensor operators of rank t calculated in the intermediate-coupling scheme. Considering that these matrix elements are

almost independent of the environment, they were taken from those determined by Lomheim and DeShazer [8] for the Nd^{3+} in $LaCl_3$. A least-squares fitting of S_{calc} to S_{meas}, treating $\Omega_{2,4,6}$ as adjustable parameters, provided the values for the three JO coefficients of Nd^{3+} in BSO. The values of $\Omega_{2,4,6}$, S_{meas}, S_{calc} and rms deviation are tabulated in table 2. The spectroscopic quality factor Ω_4/Ω_6, first introduced by Kaminskii [9], provides important spectroscopic information about the laser active medium. $\Omega_4/\Omega_6 = 0.4$ for BSO:Nd, which is in good agreement with those reported for other Nd^{3+} based laser crystals [9, 10].

Table 2. Measured (S_{meas}) and calculated (S_{calc}) absorption line strengths, JO parameters $\Omega_{2,4,6}$ (in 10^{-20} cm^2) and rms deviation for the Nd^{3+} ion in BSO:Nd.

Transition	S ($\times 10^{-20}$ cm^2)	
$^4I_{9/2} \rightarrow$	S_{meas}	S_{calc}
$^4F_{3/2}$	1.765	1.240
$^4F_{5/2}$, $^2H_{9/2}$	5.621	6.258
$^4F_{7/2}$, $^4S_{3/2}$	6.338	5.888
$^4G_{5/2}$, $^2G_{7/2}$	15.852	15.809
$\Omega_2 = 106.767$		
$\Omega_4 = 3.385$	rms deviation = 0.941	
$\Omega_6 = 8.386$		

Once the $\Omega_{2,4,6}$ JO parameters have been determined, the ED radiative emission probabilities $A(J \rightarrow J')$, corresponding to transitions from the $^4F_{3/2}$ level to the three lower $^4I_{9/2,11/2,13/2}$ manifolds, can be calculated using the following equation [11]:

$$A(J \rightarrow J') = \frac{64\pi^4 e^2}{3h(2J+1)\bar{\lambda}^3} \frac{n(n^2+2)^2}{9} S_{cal}(J \rightarrow J'). \tag{4}$$

From equations (3) and (4) it can be noted that the radiative decay rate for the transitions $^4F_{3/2} \rightarrow {}^4I_{9/2,11/2,13/2}$ depends only on the intensity parameters Ω_4 and Ω_6 because the matrix elements of rank 2 for such transitions are equal to zero [12]. The radiative lifetime for any specific excited state J can, then, be calculated using the relation:

$$\tau = \frac{1}{\sum_{J'} A(J \rightarrow J')} \tag{5}$$

where the sum is over all final states J'. The total radiative rate determined for the metastable $^4F_{3/2}$ level is 5762 s^{-1}. Therefore, the radiative lifetime is predicted to be 173.6 μs. The branching ratios can now be determined for transitions $J \rightarrow J'$ from the following relation [13]:

$$\beta_{J \rightarrow J'} = \frac{A(J \rightarrow J')}{\sum_{J'} A(J \rightarrow J')}. \tag{6}$$

The branching ratios are very important parameters to the laser designer because they characterize the possibility of attaining stimulated emission from a particular transition. As expected, the main laser emission channel $^4F_{3/2} \rightarrow {}^4I_{11/2}$ has the highest branching ratio. All these spectroscopic parameters ($A_{J' \rightarrow J'}$, $\beta_{J \rightarrow J'}$ and τ_r) are listed in table 3.

Let us now estimate the relevant spectroscopy parameters for laser applications: emission cross section and quantum efficiency. Once the branching ratios $\beta_{J \rightarrow J'}$ and the radiative lifetime τ_r are known, the spectral dependence of the stimulated emission cross section for the

Table 3. Radiative emission probabilities $A(J \rightarrow J')$, branching ratios $\beta_{J'\rightarrow J'}$ and radiative lifetime τ_r for the $^4F_{3/2} \rightarrow {}^4I_{9/2,11/2,13/2}$ transitions of the Nd^{3+} ion in BSO:Nd.

Transition	$A(J \rightarrow J')$ (s^{-1})	$\beta_{J\rightarrow J'}$	τ_r (μs)
$^4F_{3/2} \rightarrow$			173.6
$^4I_{9/2}$	1682.975	0.292	
$^4I_{11/2}$	3358.994	0.583	
$^4I_{13/2}$	719.636	0.125	

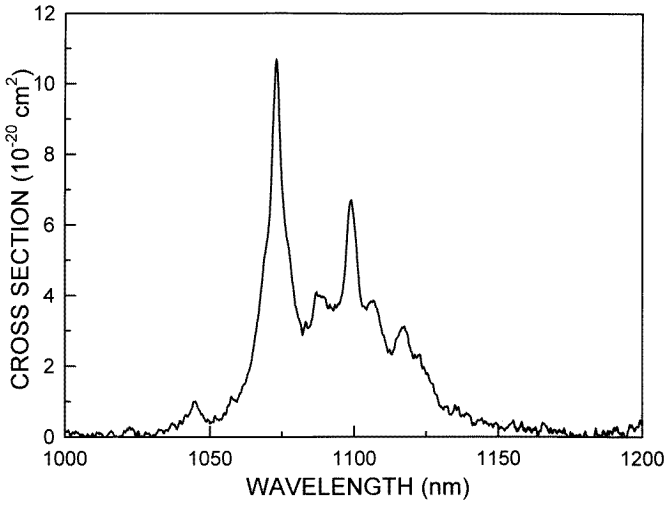

Figure 4. RT spectral dependence of the stimulated emission cross section calculated from the $^4F_{3/2} \rightarrow {}^4I_{11/2}$ emission spectrum.

main laser channel $^4F_{3/2} \rightarrow {}^4I_{11/2}$ can be determined from its RT emission spectrum according to the relation [14]:

$$\sigma = \frac{3\lambda^5 \beta_{J\rightarrow J'} I(\lambda)}{8\pi n^2 c \tau_r \int \lambda I(\lambda)\, \mathrm{d}\lambda} \tag{7}$$

where λ is the emission wavelength, $I(\lambda)$ the emission intensity as a function of wavelength and n the crystal refractive index. Figure 4 shows the spectral dependence of the stimulated emission cross section obtained from the RT emission spectrum. The peak cross section, calculated at $\lambda = 1073$ nm, resulted to be 1.07×10^{-19} cm^2, which is of the order of those reported for other Nd^{3+} based laser crystals [14, 15]. The nonradiative rate $W_{nr} = 1/\tau_f - 1/\tau_r$ of the $^4F_{3/2}$ emitting level was estimated using the value calculated for τ_r (173.6 μs) and the fluorescence lifetime measured at 11 K (106 μs). The quantum efficiency η from the $^4F_{3/2}$ emitting state was, then, found to be about 0.58, which is an acceptable value for a good laser gain of the Nd^{3+} in the BSO:Nd crystal. Moreover, the magnitude of 0.4 obtained for the spectroscopic quality parameter suggests that this compound has potential for performing stimulated emission, and therefore, it might be used in laser optical devices.

Acknowledgments

The authors wish to thank Dr Octavio Cano for his valuable assistance to identify the BSO crystal by the x-ray powder diffraction technique. This work was supported by Consejo Nacional de Ciencia y Tecnología (CONACyT) under contract No 4387-E9406. D Jaque holds a grant from Ministerio de Educación y Ciencia (España).

References

[1] Kaminskii A A 1991 *Ann. Phys., Paris* **16** 639
[2] Katsumata T, Hanamori K, Akiyama Y and Nobe Y 1995 *Mater. Res. Bull.* **30** 19
[3] Ambrazyavichyus G A, Babonas G A, Bandorev A D and Leonov E I 1981 *Opt. Spectrosc.* **51** 99
[4] Grabmaier B C and Oberschmid R 1986 *Phys. Status Solidi* a **96** 199
[5] Lomheim T S and DeShazer L G 1979 *Phys. Rev.* B **20** 4343
[6] Judd B R 1962 *Phys. Rev.* **127** 750
[7] Ofelt G S 1962 *J. Chem. Phys.* **77** 5929
[8] Lomheim T S and DeShazer L G 1978 *J. Appl. Phys.* **49** 5517
[9] Kaminskii A A 1975 *Zh. Tekh. Fiz. Pis.* **1** 256
[10] Sardar D K, Velarde-Montecinos R C and Vizcarra S 1993 *Phys. Status Solidi* a **136** 555
[11] Kaminskii A A 1981 *Springer Ser. Opt. Sci.* **14** 149
[12] Krupke W F 1974 *IEEE J. Quantum Electron.* **10** 450
[13] Caird J A and DeShaser L G 1975 *IEEE J. Quantum Electron.* **11** 97
[14] Jaque D, Capmany J, Luo Z D and García Solé J 1997 *J. Phys.: Condens. Matter* **9** 9715
[15] Burlot R, Moncargé R, Manaa H, Boulon G, Gugot Y, García Solé J and Cochet-Muchy D 1996 *Opt. Mater.* **313** 6